NATIONAL ADVISORY COMMITTEE FOR AERONAUTICS

TECHNICAL NOTE 2629

ANALYTICAL AND EXPERIMENTAL INVESTIGATION OF FULLY DEVELOPED TURBULENT FLOW OF AIR IN A SMOOTH TUBE WITH HEAT TRANSFER WITH VARIABLE FLUID PROPERTIES

By R. G. Deissler and C. S. Eian

Lewis Flight Propulsion Laboratory
Cleveland, Ohio

Washington
February 1952

NATIONAL ADVISORY COMMITTEE FOR AERONAUTICS

TECHNICAL NOTE 2629

ANALYTICAL AND EXPERIMENTAL INVESTIGATION OF FULLY DEVELOPED TURBULENT FLOW OF AIR IN A SMOOTH TUBE WITH HEAT TRANSFER WITH VARIABLE FLUID PROPERTIES

By R. G. Deissler and C. S. Eian

SUMMARY

A previous analysis of turbulent flow and heat transfer in smooth tubes with variable fluid properties was modified in order to be applicable to air which has a Prandtl number slightly less than unity (0.73). In order to verify the analysis, tests were conducted to determine local heat-transfer coefficients and friction factors for fully developed turbulent flow of air in a smooth electrically heated tube having an inside diameter of 0.87 inch and a length of 87 inches. The tests were conducted at high ratios of wall to fluid bulk temperature. Velocity and temperature profiles were measured for some conditions.

The analytically predicted results were found to agree closely with the experimental. Both the analytical and experimental results indicated that the effects of ratio of wall to bulk temperature on the Nusselt number correlation can be eliminated by evaluating the fluid properties, including density, in the Reynolds and Nusselt numbers at a temperature close to the average of the wall and bulk temperatures. In order for this correlation to apply it is necessary to assume constant Prandtl number and constant specific heat in calculating both the experimental and analytical results.

The effects of variation of shear stress and heat transfer across the tube on the velocity and temperature distributions were analytically investigated and found to be small for turbulent flow with variable fluid properties. The effects of molecular shear stress and heat transfer in the region at a distance from the wall were also investigated and found to be small.

INTRODUCTION

In an experimental investigation of average heat transfer and friction coefficients for air flowing in smooth tubes (reference 1), it

was found that the ratio of wall to fluid bulk temperature has an appreciable effect on the heat-transfer and friction correlations. A theoretical analysis given in reference 2 indicates a similar effect for local coefficients. For verification of the analysis given in reference 2, it is desirable to obtain local rather than average heat-transfer coefficients and friction factors and measurements of radial velocity and temperature distributions for large heat-transfer rates. Local rather than average coefficients are desirable because average coefficients include possible effects of flow development near the tube entrance and of heat loss at the ends of the tube.

In the investigation reported herein, which was conducted at the NACA Lewis laboratory, local heat-transfer coefficients and friction factors at high ratios of wall to bulk temperature were measured at a point in a tube where the flow was fully developed. Velocity and temperature distributions were also measured for some conditions. The analysis for flow and heat transfer with variable fluid properties given in reference 2 is modified for application to air, which has a Prandtl number slightly less than 1, and the analytically predicted results are compared with the data.

ANALYSIS FOR PRANDTL NUMBERS DIFFERING SLIGHTLY FROM ONE

The analysis given in reference 2 is for a fluid with a Prandtl number of 1. Inasmuch as air has a Prandtl number of about 0.73, the analysis is modified in this section in order to make a comparison between analytical and experimental results.

For obtaining the velocities and temperatures in the tube as functions of distance from the wall, the differential equations for shear stress and heat transfer are often written in the following form:

$$\tau = \mu \frac{du}{dy} + \rho\varepsilon \frac{du}{dy} \tag{1}$$

$$q = - k \frac{dt}{dy} - \rho c_p g \varepsilon_h \frac{dt}{dy}$$

(The symbols used in this report are defined in appendix A.)

The second equation can be rewritten as

$$\frac{q}{c_p g} = - \left(\frac{\mu}{Pr} + \rho\varepsilon_h \right) \frac{dt}{dy} \tag{2}$$

In the preceding equations, ε and ε_h are the coefficients of eddy diffusivity for momentum and heat transfer, respectively, the values for which are dependent on the amount and kind of turbulent mixing at a point.

Assumptions. - The following assumptions are made in the use of equations (1) and (2) for obtaining velocity and temperature distributions with heat transfer:

(1) The eddy diffusivities for momentum and heat transfer ε and ε_h are equal. Previous analyses for flow in tubes based on this assumption yielded heat-transfer coefficients and friction factors that agree with experiment.

(2) The expressions for eddy diffusivity that are found in reference 3 to apply to flow without heat transfer apply also to flow with heat transfer with variable fluid properties. These expressions are

$$\varepsilon = n^2 uy \tag{3}$$

for flow close to the wall $(y+ < 26)$ and the Kármán relation

$$\varepsilon = \kappa^2 \frac{\left(\frac{du}{dy}\right)^3}{\left(\frac{d^2u}{dy^2}\right)^2} \tag{4}$$

for flow at a distance from the wall $(y+ > 26)$, where n and κ are experimental constants having the values 0.109 and 0.36, respectively.

(3) The variations across the tube of the shear stress τ and the heat transfer per unit area q have a negligible effect on the velocity and temperature distributions. The effect of these variations will be investigated in appendix B and in the section "Predicted Effect of Variation of Shear Stress and Heat Transfer Across Tube."

(4) The molecular shear stress and heat-transfer terms in equations (1) and (2) can be neglected in the region at a distance from the wall. The effect of these terms will be investigated in appendix C and in the section "Predicted Effect of Molecular Shear Stress and Heat Transfer in Region at a Distance from Wall."

(5) The static pressure can be considered constant across the tube.

(6) The Prandtl number and specific heat can be considered constant with temperature variation. The variations with temperature of the specific heat and the Prandtl number of gases are of a lower order of magnitude than the variations of viscosity, thermal conductivity, and density.

Flow close to wall. - For obtaining the velocity and temperature distributions close to a smooth wall, the expression for ε from equation (3) is substituted into equations (1) and (2) to give

$$\tau_0 = (\mu + n^2 \rho u y) \frac{du}{dy}$$

and

$$\frac{q_0}{c_p g} = - \left(\frac{\mu}{Pr} + n^2 \rho u y \right) \frac{dt}{dy}$$

where ε and ε_h have been assumed equal (assumption (1)) and τ and q have been replaced by τ_0 and q_0 (assumption (3)). With substitution of the dimensionless quantities u^+, y^+, and β these equations become

$$1 = \left(\frac{\mu}{\mu_0} + \frac{\rho}{\rho_0} n^2 u^+ y^+ \right) \frac{du^+}{dy^+} \tag{5}$$

and

$$\beta = - \left(\frac{\mu/\mu_0}{Pr} + \frac{\rho}{\rho_0} n^2 u^+ y^+ \right) \frac{d(t/t_0)}{dy^+} \tag{6}$$

From viscosity data it is found that μ/μ_0 can be represented approximately by $(t/t_0)^d$; and from the assumption of constant static pressure (assumption (5)) and the perfect gas law, ρ/ρ_0 can be replaced by t_0/t. From the definitions of β and t^+

$$\frac{t}{t_0} = 1 - \beta t^+ \tag{7}$$

Equations (5) and (6) then become

$$1 = \left[(1-\beta t^+)^d + \frac{1}{(1-\beta t^+)} n^2 u^+ y^+ \right] \frac{du^+}{dy^+} \tag{8}$$

and

$$1 = \left[\frac{(1-\beta t^+)^d}{Pr} + \frac{1}{1-\beta t^+} n^2 u^+ y^+ \right] \frac{dt^+}{dy^+} \tag{9}$$

Equations (8) and (9) can be written in integral form as

$$u^+ = \int_0^{y^+} \frac{dy^+}{(1-\beta t^+)^d + \frac{n^2 u^+ y^+}{1-\beta t^+}} \tag{10}$$

and

$$t^+ = \int_0^{y^+} \frac{dy^+}{\frac{(1-\beta t^+)^d}{Pr} + \frac{n^2 u^+ y^+}{1-\beta t^+}} \tag{11}$$

Equations (10) and (11) can be solved simultaneously by iteration, that is, assumed values for u^+, y^+, and t^+ are substituted into the right sides of the equations and new values of u^+ and t^+ are calculated by numerical integration. These new values are then substituted into the right sides of the equations and the process is repeated until the values of u^+ and t^+ corresponding to each value of y^+ do not change appreciably. Equations (10) and (11) give the relations between u^+, t^+, and y^+ for various values of the heat-transfer parameter β for flow close to a wall.

Flow at a distance from wall. - By making use of assumptions (1), (2), (3), (4), and (6), equations (1) and (2) can be written in dimensionless form for flow at a distance from the wall as

$$1 = \frac{\rho}{\rho_0} \kappa^2 \frac{(du^+/dy^+)^3}{(d^2u^+/dy^{+2})^2} \frac{du^+}{dy^+} \tag{12}$$

and

$$1 = \frac{\rho}{\rho_0} \kappa^2 \frac{(du^+/dy^+)^3}{(d^2u^+/dy^{+2})^2} \frac{dt^+}{dy^+} \tag{13}$$

Dividing equation (12) by equation (13) and integrating result in

$$\int_{t_1^+}^{t^+} dt^+ = \int_{u_1^+}^{u^+} du^+$$

or

$$t^+ - t_1^+ = u^+ - u_1^+ \tag{14}$$

where t_1^+ and u_1^+ are the values of t^+ and u^+ at y_1^+, which is the lowest value of y^+ for which equations (12) and (13) apply. Then

$$\frac{t}{t_0} = 1 - (u^+ - u_1^+ + t_1^+)\beta \tag{15}$$

or, from assumption (5) and the perfect gas law,

$$\frac{\rho}{\rho_0} = \frac{1}{1 - (u^+ - u_1^+ + t_1^+)\beta} \tag{16}$$

On substituting equation (16) in equation (12) there results

$$1 - (u^+ - u_1^+ + t_1^+)\beta = \kappa^2 \frac{(du^+/dy^+)^4}{(d^2u^+/dy^{+2})^2} \tag{17}$$

One integration of equation (17) gives

$$C_1\beta \frac{du^+}{dy^+} = -e^{\frac{2\kappa}{\beta}\sqrt{1 - \beta(u^+ - u_1^+ + t_1^+)}} \tag{18}$$

where the negative sign was selected in taking the square root in order to make κ positive. Integration of equation (18) gives

$$y^+ = -\frac{C_1\beta^2}{2\kappa^2} e^{-\frac{2\kappa}{\beta}\sqrt{1 - \beta(u^+ - u_1^+ + t_1^+)}} \left[\frac{2\kappa}{\beta}\sqrt{1 - \beta(u^+ - u_1^+ + t_1^+)} + 1\right] + C \tag{19}$$

As the wall is approached, the velocity gradient becomes very large compared with that at a distance from the wall so that dy^+/du^+ approaches zero as y^+ approaches zero. If dy^+/du^+ is substituted from equation (18) into equation (19) and dy^+/du^+ is set equal to zero when y^+ and u^+ equal zero, C equals zero. To determine C_1, set $u^+ = u_1^+$ when $y^+ = y_1^+$. Then

$$C_1 = \frac{2\varkappa^2 y_1^+}{\beta^2 e^{-\frac{2\varkappa}{\beta}\sqrt{1-\beta t_1^+}}\left(\frac{2\varkappa}{\beta}\sqrt{1-\beta t_1^+}+1\right)}$$

and

$$y^+ = \frac{y_1^+ e^{-\frac{2\varkappa}{\beta}\sqrt{1-\beta(u^+-u_1^++t_1^+)}}\left[\frac{2\varkappa}{\beta}\sqrt{1-\beta(u^+-u_1^++t_1^+)}+1\right]}{e^{-\frac{2\varkappa}{\beta}\sqrt{1-\beta t_1^+}}\left(\frac{2\varkappa}{\beta}\sqrt{1-\beta t_1^+}+1\right)} \quad (20)$$

Equation (20) gives the relation between u^+ and y^+ for various values of β for flow far from the wall. The parameter t^+ and thus the temperature distribution can be calculated from equation (14). For a Prandtl number of 1, $t_1^+ = u_1^+$; and equation (20) reduces to the equation for a Prandtl number of 1 given in reference 2. For $\beta = 0$ equation (20) is indeterminate. For this case β is set equal to zero in equation (17) before integrating, and the well-known logarithmic equation is obtained:

$$u^+ = \frac{1}{\varkappa}\log_e y^+ + C$$

Nusselt number, Reynolds number, and friction factor. - It can easily be shown from the definitions of the quantities involved (see reference 2) that the Nusselt number, Reynolds number, and friction factor with the fluid properties evaluated at the wall temperature are given by

$$Nu_0 = \frac{2r_0^+ Pr}{t_b^+} \quad (21)$$

$$Re_0 = 2u_b^+ r_0^+ \quad (22)$$

$$f_0 = \frac{2}{u_b^{+2}} \quad (23)$$

where

$$t_b^+ = \frac{\int_0^{r_0^+} \frac{t^+u^+(r_0^+-y^+)}{1-\beta t^+}\,dy^+}{\int_0^{r_0^+} \frac{u^+(r_0^+-y^+)}{1-\beta t^+}\,dy^+} \tag{24}$$

and

$$u_b^+ = \frac{2}{r_0^{+2}}\int_0^{r_0^+} u^+(r_0^+-y^+)dy^+ \tag{25}$$

The relations between u^+, y^+, and t^+ are calculated from the equations given in the two preceding sections.

The Nusselt number, Reynolds number, and friction factor with the fluid properties evaluated at some temperature in the fluid other than the wall temperature can be found by using the following equation for t_b/t_0:

$$\frac{t_b}{t_0} = \frac{\int_0^{r_0^+} u^+(r_0^+-y^+)dy^+}{\int_0^{r_0^+} \frac{u^+(r_0^+-y^+)}{1-\beta t^+}\,dy^+} \tag{26}$$

Both the thermal-conductivity ratio and the viscosity ratio are equal to the temperature ratio raised to the exponent d inasmuch as the specific heat and Prandtl number are assumed constant (assumption (6)).

Although the preceding analysis was carried out for the case where the compressibility effects due to high velocities can be neglected, it is shown in reference 2 that the same correlations apply, in general, to flow at high subsonic velocities. For the latter case (except for very small temperature differences) it is necessary only to replace the static bulk temperature by the total bulk temperature in the definition of the heat-transfer coefficient h.

APPARATUS

A schematic diagram of the test section and associated equipment is shown in figure 1. Compressed air first passes through a filter and then into an alumina-type air dryer. From the dryer the air flows through one of four orifices selected remotely by orifice selection valves and then through valves which automatically control the flow rate. From the control valves the air flows into a surge tank, then to the inlet mixing tank, through the test section, and into the outlet mixing tank from which it is discharged to the atmosphere through a pressure regulating valve.

Electric power is supplied to the heater tube from a 208-volt 60-cycle supply through an autotransformer and a step-down transformer with maximum secondary voltages of either 15 or 25 volts. The low-voltage leads of the step-down transformer are connected to the flanges on the ends of the test section by copper bus bars. The capacity of the electric equipment is 100 kilovolt-amperes. Additional heat to compensate for end losses is supplied to each end of the heater tube where guard heater coils of nichrome wire are wrapped around the cone-shaped heater-tube flanges. Individual control of the 110-volt 60-cycle supply to each end of the tube is obtained by variable transformer with capacities of 1 kilovolt-ampere.

Test Section

The test section, shown in detail in figure 2, is a commercially smooth Inconel tube having an inside diameter of 0.87 inch and an outside diameter of 1.25 inches with a sharp right-angle entrance. Steel flanges with cone-shaped centers welded to the tube at each end provide electrical contact with the transformer leads from the power supply. The tube, which is thermally insulated by a 5-inch thickness of high temperature quartz wool, acts as a heating element with an effective heat-transfer length of 87 inches. Static pressures are measured through 0.03-inch holes drilled in the tube at the positions shown in figure 2. Outside tube-wall temperatures are measured by chromel-alumel thermocouples (two thermocouples located 180° apart at each of 21 stations and one near each end of the tube) and a self-balancing indicating-type potentiometer. Air total temperatures are measured by thermocouples located in the central passages of the inlet and outlet mixing tanks of the test section as shown in figure 1. The inlet mixing tank consists of two concentric passages so arranged that the air makes two passes through the tank before entering the test section, while the outlet mixing tank is comprised of four concentric tanks. The passage of the air through the central chamber and concentric passages prevents radiation errors in the temperature measurements. Baffles are provided in the central passages to insure thorough mixing of the air before its temperature is measured.

Total-Pressure Measurements

An opening for taking total-pressure measurements across the tube is located 6 inches from the exit of the tube as shown in figure 2. A hole having a 0.15-inch diameter through which a total-pressure probe enters the tube was drilled in the tube wall at right angles to the static-pressure taps. A probe actuator to move the probe and measure its distance into the tube was fitted to a 6-inch length of tubing at the opening. The location of the total-pressure probe with respect to the opening is shown in figure 2(b). The probe tip has a flat opening with a height of 0.004 inch and a 0.002-inch wall and is made so that the tip just clears the edge of the 0.15-inch hole in the test section. The total projected area of the probe in the direction of flow with the tip at the center of the tube is about $1\frac{1}{2}$ percent of the area of the tube, but the effective blocking area at the tip is considerably less because the main portion of the probe is downstream of the tip.

Total-Temperature Measurements

The same opening in the tube used for taking total-pressure measurements is used for taking total-temperature measurements. Figure 2(c) shows the location of the total-temperature probe with respect to the opening in the tube. One of the two prongs of the probe is made of chromel while the other is made of alumel. The thermocouple of the probe consists of 0.001-inch chromel and alumel wire butt-welded between the prongs which were 0.07-inch apart. Temperatures as measured by the probe were read on a self-balancing indicating-type potentiometer.

METHODS

Test Procedure

Preliminary runs with no air flow were first made to determine both heat loss through the test-section insulation and required power settings for the end heaters. The tube was heated to various temperatures by adjusting the electrical power input to the tube, and the power settings for the end heaters were adjusted to give a uniform wall temperature for each run.

For each test run the flow control was adjusted to give the desired flow rate and the electric-power control for the tube was set to give the desired tube-wall temperature. The power settings to be used for the end heaters at each temperature were determined from the preliminary runs. For the runs made the tube-wall temperature near the exit varied between 300° and 1500° F, and the Reynolds number with fluid properties based on the bulk temperature varied between 8000 and 500,000. The maximum Mach number was about 0.6.

The following quantities were measured for each run: air flow, static pressures at the wall, outside tube-wall temperatures, inlet and outlet total bulk-air temperature, and electrical-power input to the tube. Total-pressure and temperature surveys at a section 6 inches from the exit of the tube where the flow was practically fully developed were taken during some of the tests. Measurements were taken at points between the wall in which the probe opening was located and the center of the tube. Measurements made near the opposite wall were inaccurate because of disturbance due to the probe. Total-pressure surveys were taken for tube-wall temperatures up to 1500° F, whereas total-temperature surveys were made only at low wall temperatures (300° F) because of the delicacy of the temperature probe.

Reduction of Experimental Data

Local heat-transfer rate. - The local heat-transfer rate per unit area from the tube to the air at a cross-section of the tube was calculated from

$$q_0 = \left(\frac{w\,\Delta H}{S_{ave}}\right)\left(\frac{G_{loc} - L_{loc}}{G_{ave} - L_{ave}}\right) \tag{27}$$

where the change of enthalpy ΔH was obtained from the bulk total temperatures of the air at the inlet and outlet of the tube. The heat generation per square foot of tube area G was obtained by measurement of electric current and tube resistance and the heat loss L was determined by heating the tube to various temperatures with no air flowing. The quantities G, L, and S are all functions of tube temperature; the subscript loc means that the quantities were determined at the local tube temperature, whereas the subscript ave means that they were determined at the average tube temperature. The quantity in the first parenthesis is the average heat transfer per unit area; the quantity in the second parenthesis is a correction factor for local heat transfer.

The local heat-transfer rate q_0 was determined from equation (27) rather than from $G_{loc} - L_{loc}$ because the measurements of inlet and outlet air temperature were, in general, more accurate than those of tube resistance and heat loss. The use of this equation also reduces errors due to possible nonequilibrium conditions. The quantity in the second parenthesis in the equation did not vary greatly from 1 for most of the tests.

Inside tube-wall and local bulk temperatures. - The inside tube-wall temperature t_0 was obtained from the measured outside tube-wall temperature t_a by the following equation derived in reference 4:

$$t_0 = t_a - \frac{q_0 r_0}{K_t}\left[\frac{r_a^2}{r_a^2 - r_0^2}\log_e\left(\frac{r_a}{r_0}\right) - \frac{1}{2}\right] \tag{28}$$

In equation (28) the assumptions are made that heat is generated uniformly across the tube wall thickness and that the heat flow at every point in the tube is radially inward. For the present tests the radial temperature drop through the tube wall was very small compared with the difference between the inside wall and the air bulk temperature.

The local total bulk-air temperature at a point was obtained by subtracting from the measured bulk temperature at the tube exit the temperature change produced by the heat added to the air in the portion of the tube between the exit and the point in question.

Physical properties of air. - In order to compare the experimental results with the analysis given in reference 2, the viscosity and thermal conductivity were both assumed to be proportional to $t^{0.68}$. The specific heat and Prandtl number were assumed not to vary with temperature. Substantially different results would be obtained if a different variation of thermal conductivity with temperature were used. A conductivity proportional to $t^{0.85}$ is sometimes given in the literature, but the actual variation of conductivity with temperature has not been experimentally determined at high temperatures.

Shear stress. - The shear stress at the wall for fully developed flow is related to the friction-pressure gradient by the equation

$$\tau_0 = -\frac{D}{4}\left(\frac{dp}{dx}\right)_{fr} \tag{29}$$

The friction-pressure gradients were obtained by subtracting calculated momentum-pressure gradients from the measured static-pressure gradients along the tube; the momentum-pressure gradients were calculated from

$$\left(\frac{dp}{dx}\right)_{mom} = \frac{w^2}{\rho_b{}^2 A^2 g^2}\frac{d\rho_b}{dx} \tag{30}$$

Equation (30) is exact only when the velocity profile is uniform; the effect of nonuniform velocity profile on calculated shear stress was checked for turbulent flow and was found to be negligible for the present tests. In equation (30) ρ_b was found from the perfect gas law

$$p = \rho_b g R t_b \tag{31}$$

and $d\rho_b/dx$ was obtained by differentiation of the perfect gas law to be

$$\frac{d\rho_b}{dx} = \frac{1}{gRt_b}\frac{dp}{dx} - \frac{p}{gRt_b^2}\frac{dt_b}{dx} \tag{32}$$

In this equation t_b was found from the following relation obtained from the equations of energy, continuity, and state:

$$t_b = \frac{-1 + \sqrt{1 + 2\dfrac{w^2 R^2 T_b}{gJ\, c_p A^2 p^2}}}{\dfrac{w^2 R^2}{gJ\, c_p A^2 p^2}} \tag{33}$$

This equation can be more conveniently used for calculation purposes if the radical is expanded in a binominal series. The quantity dt_b/dx was obtained by differentiating the expanded equation for t_b with respect to x:

$$\frac{dt_b}{dx} = \frac{dT_b}{dx} - \frac{w^2 R^2}{gJ\, c_p A^2}\frac{pT_b\dfrac{dT_b}{dx} - T_b^2\dfrac{dp}{dx}}{p^3} +$$

$$\frac{1}{2}\left(\frac{w^2 R^2}{gJ\, c_p A^2}\right)^2 \frac{3pT_b^2\dfrac{dT_b}{dx} - 4T_b^3\dfrac{dp}{dx}}{p^5} - \cdots \tag{34}$$

where

$$\frac{dT_b}{dx} = \frac{\pi D q_0}{w c_p} \tag{35}$$

The static-pressure gradients in equations (32) and (34) were graphically determined by plotting pressure against distance along the tube and drawing a tangent to the curve at the point in question.

Velocity distributions. - For low air flow rates, incompressible flow theory was used; the velocities were calculated from the equation

$$P - p = \frac{1}{2} \rho u^2 \tag{36}$$

where ρ was found from the perfect gas law $p = \rho g R t$ and t was taken equal to the total temperature. In this and in all of the succeeding calculations, the static pressure was assumed to be uniform across the tube.

For Mach numbers greater than 0.2, velocities were calculated from the relation

$$\frac{P}{p} = \left(1 + \frac{\gamma - 1}{\gamma} \frac{u^2}{2gRt}\right)^{\frac{\gamma}{\gamma - 1}} \tag{37}$$

where

$$t = T \left(\frac{p}{P}\right)^{\frac{\gamma - 1}{\gamma}}$$

For both low and high Mach numbers the total temperature in the equations was obtained from the theoretical curves in figure 3. (Fig. 3 is applied to compressible flow by replacing t^+ by T^+. This procedure is legitimate for Prandtl numbers close to 1.)

RESULTS AND DISCUSSION

Predicted Temperature and Velocity Distributions

(Prandtl Number = 0.73)

Temperature and velocity distributions for a Prandtl number of 0.73 as calculated from equations (10), (11), (20), and (14) are plotted in figures 3 and 4. The values for the constants ($n = 0.109$ and $\varkappa = 0.36$), which are found in reference 3 from the experimental data for flow without heat transfer, are used for plotting the equations. In reference 3 it is found that the equation derived for flow close to a wall without heat transfer agrees closely with the data for y^+ less than 26 and that the equation for flow at a distance from a wall without heat transfer fits the data for y^+ greater than 26. For plotting the present equations for flow with heat addition to the gas, the same limits of applicability for the equations for flow close to a wall and at a distance from a wall are used. It can be seen from the figures that the exact point of intersection of the curves representing the two equations is not critical, especially for high values of β, inasmuch as the slopes of the two curves at their intersection do not differ greatly.

The exponent d in the equations was found from viscosity data for air to have an average value of 0.68 for temperatures between 0° and 2000° F. Although this value was obtained specifically for air, the values of d for most common gases do not vary greatly from this value, so that the curves plotted should be applicable to most gases with Prandtl numbers close to 0.73.

The plots of the equations in figures 3 and 4 indicate that t^+ and u^+ are not equal as was the case for a Prandtl number of 1 (reference 2). Both profiles, however, show trends with increasing values of the heat-transfer parameter β which are similar to those found in reference 2 for a Prandtl number of 1.

Nusselt Numbers

In figures 5, 6, and 7, experimental and predicted Nusselt numbers for air (Pr = 0.73) are plotted against Reynolds numbers for various values of the heat-transfer parameter β. The experimental Nusselt numbers and Reynolds numbers were obtained at a point 6 inches from the exit of the tube where the flow was practically fully developed and were calculated from the definitions of Reynolds number, Nusselt number, and heat-transfer coefficient based on total-temperature difference, as given in the list of symbols. The predicted Nusselt and Reynolds numbers were obtained from the equations given in the analysis for Prandtl numbers differing slightly from 1 and from the plots in figures 3 and 4.

In figure 5 the physical properties, including density, in the Reynolds number and Nusselt number are evaluated at the static bulk temperature. Both the experimental and predicted Nusselt numbers at a given Reynolds number show a decrease with increasing values of β or of ratio of wall to bulk temperature. In figure 6 the physical properties, including density, in the Reynolds and Nusselt numbers are evaluated at the wall temperature. For this case, both the experimental and predicted Nusselt numbers at a given Reynolds number increase with increasing β. In figure 7 the properties in the Reynolds and Nusselt numbers are evaluated at $t_{0.4}$, which is slightly closer to the bulk temperature than the average of the wall and bulk temperatures. It is observed that the effect of β or of ratio of wall to bulk temperature on both the experimental and predicted Nusselt numbers is practically eliminated when the properties are evaluated at this temperature. The data follow the predicted line very closely for Reynolds numbers above 15,000. For low Reynolds numbers the separation of the data from the predicted line is probably caused by a partial transition from turbulent to laminar heat transfer, which was not considered in the analysis. The same trend at low Reynolds numbers was also observed in the data given in reference 1. It is seen that the transition region extends to higher Reynolds numbers for heat transfer than for friction.

It should be emphasized that in order for the foregoing correlation to hold, the same assumptions for the variation of physical properties with temperature must be made for calculating the experimental results as were made in the analysis: constant specific heat and both thermal conductivity and viscosity proportional to $t^{0.68}$. If the conductivity had been assumed proportional to $t^{0.85}$ as sometimes given in the literature, the effects of ratio of wall to bulk temperature on the Nusselt number correlation would have been eliminated by evaluating the fluid properties at a temperature close to the wall temperature. The actual variation of the thermal conductivity of air with temperature has not been experimentally determined at high temperatures. In reference 1 it is found that the best correlation of average heat-transfer coefficients for both heating and cooling was obtained by assuming the thermal conductivity proportional to $t^{0.5}$ and evaluating the properties, including density, in the Reynolds and Nusselt numbers at the average of the wall and bulk temperatures. If a constant rather than a variable specific heat had been used in reference 1, it would have been necessary to use a conductivity proportional to $t^{0.6}$ in order to eliminate the effect of ratio of wall to bulk temperature. The data for average heat-transfer coefficients given in reference 1 are therefore in substantial agreement with the present data and analysis for local heat-transfer coefficients. For the range of ratios of wall to bulk temperatures used in the present tests, as good a correlation could be obtained by evaluating the properties at the average of the wall and bulk temperatures as by evaluating them at $t_{0.4}$.

Although extensive data were not obtained in the low Reynolds number range at high ratios of wall to bulk temperature, the data taken indicate that in this range the effects of β are more nearly eliminated by evaluating the properties at the bulk temperature than at $t_{0.4}$. This is in agreement with the analysis given in reference 5, where it is shown that for laminar flow the properties should be evaluated at a temperature between the bulk temperature and the temperature at the center of the tube. It would be expected that in the transition region the properties should be evaluated at temperatures between this temperature and $t_{0.4}$.

Friction Factors

In figure 8, experimental and predicted friction factors for air are plotted against Reynolds numbers for various values of the heat-transfer parameter β. The physical properties, including density, in the friction factors and Reynolds numbers in the figure are evaluated at $t_{0.4}$. The experimental friction factors and Reynolds numbers were obtained at a point 6 inches from the exit of the tube and were calculated from the definitions of friction factor and Reynolds number given in the list of symbols.

The plot of predicted friction factors given in figure 8 indicates that the effects of β or of ratio of wall to bulk temperature are nearly eliminated by evaluating the properties at $t_{0.4}$. The data at high Reynolds numbers also indicate that the effects of ratio of wall to bulk temperature are eliminated by evaluating the properties at that temperature. The data agree closely with the predicted line in the high Reynolds number range. At lower Reynolds numbers the agreement is not as good, although it may be within the experimental accuracy. Measurements of friction factors are, in general, much less accurate than those of heat-transfer coefficients because of difficulties in measuring static-pressure gradients. In reference 1 it is found that some of the data for average friction factors at low Reynolds numbers lie both below and above the predicted line in figure 8, when the fluid properties are evaluated at the average of the wall and bulk temperatures.

Velocity Distributions

Experimental and predicted velocity distributions for various values of β are shown in figure 9. Rectangular rather than semilogarithmic coordinates are used inasmuch as data are not shown for flow close to the wall; these data are not shown because the distributions were measured at high Reynolds numbers where the severe velocity gradients and the presence of the hole in the tube wall make the accuracy of the measurements doubtful.

It can be seen that the experimental and predicted values are in substantial agreement although there is some scatter in the data. Inasmuch as the experimental distributions were measured in the high Reynolds number range where the experimental friction factors fell on the predicted line, the agreement between the experimental and predicted velocity distributions might be expected. It appears that measurement of velocity distributions with heat transfer yields little information in addition to that obtained by measurement of friction factors and heat-transfer coefficients other than possible information concerning changes in shape of the velocity profile with heat transfer. However, as indicated in figure 10, changes in profile shape should be very small over most of the tube cross section for the range of values of β obtained in the tests (0 to 0.028) and probably could not be measured experimentally.

Temperature Distributions

Experimental and predicted temperature distributions are plotted in figure 11. Data for temperature distributions close to the wall are shown only at low flow rates because at high flow rates the severe velocity and temperature gradients and the presence of the hole in the

tube wall make the accuracy of the measurements doubtful. The distributions shown for the region close to the wall may be subject to errors due to conduction along the thermocouple probe prongs inasmuch as the velocities in that region are very small. Temperature distributions were not measured for high values of β or of ratio of wall to bulk temperature because of the delicacy of the temperature probe and because it appeared that such measurements would not yield appreciable information beyond that obtained by measuring heat-transfer coefficients and friction factors at high values of β. Changes in temperature profile shape with heat transfer should be small as in the case of velocity profile (fig. 10).

It is seen in figure 11 that the experimental temperature distributions agree fairly well with those predicted except in the low Reynolds number region where transition from turbulent to laminar heat transfer is taking place. This separation of data from the predicted line at low Reynolds numbers is not present in the velocity distribution data given in reference 3, so that it appears that the eddy diffusivities for heat and momentum transfer cannot be considered equal in the low Reynolds or Peclet number range. The eddy diffusivity for heat transfer in this range is probably a function of the thermal diffusivity $k/(\rho g c_p)$ as well as of the flow conditions.

Predicted Effect of Variation of Shear Stress and Heat Transfer Across Tube

A comparison between equations (7B) and (8B) (appendix B), which take into account the variation in shear stress and heat transfer across the tube, and the equations from reference 2, which assume uniform shear stress and heat transfer, is shown in figure 12 for various values of the heat-transfer parameter β. The intersection of the curves for flow close to and far from the wall is taken at $y^+ = 30$ rather than 26 for variable shear stress in order to make the mean deviation of equations (7B) and (8B) from those given in reference 2 a minimum. It is seen that the effect of variable shear stress and heat transfer on the velocity distributions is small and is probably within the accuracy of flow and pressure measurements. The effect is greater for heat extraction (negative β) than for heat addition to the gas.

Although the preceding calculations were carried out for a Prandtl number of 1, it is evident that the effects of variable shear stress and heat transfer would also be small for a Prandtl number of 0.73.

Predicted Effect of Molecular Shear Stress and Heat Transfer in Region at a Distance from Wall

The results of the analysis of the effect of molecular shear stress and heat transfer in the region at a distance from the wall are shown in figures 13 and 14. For the region close to the wall, the curves were calculated from the equation given in reference 2; for flow close to a wall for a Prandtl number of 1 and for the region at a distance from the wall, the curves were calculated from equations (3C) and (4C) (appendix C). The three experimental constants involved in the plots are n, $\varkappa$, and y_1^+, all of which are determined from experimental data for adiabatic turbulent flow from reference 3. The values for n and $\varkappa$ are taken directly from reference 3, and y_1^+ is so determined that the curve for $\beta = 0$ agrees with the data for adiabatic flow. The slope v_1 in equation (3C) is set equal to the slope of the equation for flow close to the wall at y_1^+ ($v_1 = 0.233$ for $\beta = 0.05$).

By including the molecular shear stress and heat transfer in the equation for flow at a distance from the wall, the region of applicability of the Kármán similarity expression is extended from $y^+ > 26$ to $y^+ > 16$. At $y^+ = 16$, the curve joins smoothly with the curve for flow close to the wall with no discontinuity in slope, that is, the eddy diffusivity as determined from the equations is continuous from the wall to the center of the tube.

A comparison of the curves plotted with the molecular shear stress and heat transfer in the region at a distance from the wall neglected with those plotted with these factors considered in this region is presented in figure 14. Only a small difference in results is obtained. As a result of this agreement, the heat-transfer coefficients and friction factors will also be unaffected so that the molecular shear stress and heat transfer can be neglected with good approximation in the region at a distance from the wall. Although the preceding calculations were carried out for a Prandtl number of 1, it is evident that the same conclusions would hold for a Prandtl number of 0.73.

SUMMARY OF RESULTS

The following results were obtained from the analytical and experimental investigation of fully developed turbulent flow and heat transfer in smooth tubes with variable fluid properties:

1. Substantial agreement was obtained between experimental and analytically predicted heat transfer and friction correlations as well as velocity and temperature distributions.

2. The best check of the analysis was obtained by measurement of local heat-transfer coefficients. Both the experimental and analytical results indicated that, for Reynolds numbers above 15,000, the effects of ratio of wall to bulk temperature on the Nusselt number correlation can be eliminated by evaluating the fluid properties, including density, in the Reynolds and Nusselt numbers at a temperature close to the average of the wall and bulk temperatures. In using the preceding result for calculations, it is important to use thermal conductivities and viscosities both proportional to the absolute temperature raised to the 0.68 power and constant specific heat.

3. The analysis indicated that the effect of variation of shear stress and heat transfer across the tube on the velocity and temperature distributions for turbulent flow with variable fluid properties is slight.

4. The analysis indicated that the effect of molecular shear stress and heat transfer in the region at a distance from the wall is slight for turbulent flow with variable fluid properties.

Lewis Flight Propulsion Laboratory
National Advisory Committee for Aeronautics
Cleveland, Ohio, October 18, 1951

APPENDIX A

SYMBOLS

The following symbols are used in this report:

A	cross-sectional area based on inside diameter of tube, sq ft
C, C_1	constants of integration
c_p	specific heat of fluid at constant pressure, Btu/(lb)($^\circ$F)
D	inside diameter of tube, ft
d	exponent that describes variation of viscosity of fluid with temperature
G	heat generated in tube, Btu/(sec)(sq ft)
g	acceleration due to gravity, 32.2 ft/sec^2
H	enthalpy, Btu/lb
h	heat-transfer coefficient, $\frac{q_0}{T_0 - T_b}$ for compressible fluid or $\frac{q_0}{t_0 - t_b}$ for incompressible fluid, Btu/(sec)(sq ft)($^\circ$F)
J	mechanical equivalent of heat, 778 ft-lb/Btu
K_t	thermal conductivity of tube material, (Btu)(ft)/(sec)(sq ft)($^\circ$F)
k	thermal conductivity of fluid, (Btu)(ft)/(sec)(sq ft)($^\circ$F)
k_b	thermal conductivity of fluid evaluated at t_b, (Btu)(ft)/(sec)(sq ft)($^\circ$F)
k_0	thermal conductivity of fluid evaluated at wall, (Btu)(ft)/(sec)(sq ft)($^\circ$F)
$k_{0.4}$	thermal conductivity of fluid evaluated at $t_{0.4}$, (Btu)(ft)/(sec)(sq ft)($^\circ$F)
L	heat loss through insulation, Btu/(sec)(sq ft)
n	constant
P	total pressure, lb/sq ft absolute

p	static pressure, lb/sq ft absolute
q	rate of heat transfer toward tube center per unit area, Btu/(sec)(sq ft)
q_0	rate of heat transfer at inside wall toward tube center per unit area, Btu/(sec)(sq ft)
R	perfect gas constant, ft-lb/(lb)($^\circ$R)
r_0	inside tube radius, ft
r_a	outside tube wall radius, ft
S	inside surface area of tube, sq ft
T	total temperature, $^\circ$R
T_b	bulk or average total temperature of fluid at cross section of tube, $^\circ$R
T_0 or t_0	absolute wall temperature, $^\circ$R
t	absolute static temperature, $^\circ$R
t_b	bulk or average static temperature of fluid at cross section of tube, $^\circ$R
$t_{0.4}$	film temperature, $0.4(t_0 - t_b) + t_b$, $^\circ$R
u	time average velocity parallel to axis of tube, ft/sec
u_b	bulk or average velocity at cross section of tube, ft/sec
w	fluid-flow rate, lb/sec
x	axial distance from tube entrance, ft
y	distance from tube wall, ft
γ	ratio of specific heats
ε	coefficient of eddy diffusivity for momentum, sq ft/sec
ε_h	coefficient of eddy diffusivity for heat, sq ft/sec
κ	Kármán constant

μ absolute viscosity of fluid, (lb)(sec)/sq ft

μ_b absolute viscosity of fluid evaluated at t_b, (lb)(sec)/sq ft

μ_0 absolute viscosity of fluid at wall, (lb)(sec)/sq ft

$\mu_{0.4}$ absolute viscosity of fluid evaluated at $t_{0.4}$, (lb)(sec)/sq ft

ρ mass density, lb-sec^2/ft^4

ρ_b bulk or average density at cross section of tube, lb-sec^2/ft^4

ρ_0 mass density of fluid at wall, lb-sec^2/ft^4

$\rho_{0.4}$ density of fluid evaluated at $t_{0.4}$, lb-sec^2/ft^4

τ shear stress in fluid, lb/sq ft

τ_0 shear stress in fluid at wall, lb/sq ft

Subscripts:

fr on friction-pressure gradient

mom on momentum-pressure gradient

Dimensionless parameters:

β heat-transfer parameter, $\dfrac{q_0\sqrt{\tau_0/\rho_0}}{c_p g \tau_0 t_0}$

f_0 friction factor with density evaluated at t_0, $-\dfrac{D(dp/dx)_{fr}}{2\rho_0 u_b^2} = \dfrac{2\tau_0}{\rho_0 u_b^2}$

$f_{0.4}$ friction factor with density evaluated at $t_{0.4}$

M Mach number, $\dfrac{u}{\sqrt{\gamma g R t}}$

Nu_b Nusselt number with thermal conductivity evaluated at t_b, $\dfrac{hD}{k_b}$

Nu_0 Nusselt number with thermal conductivity evaluated at t_0

$Nu_{0.4}$ Nusselt number with thermal conductivity evaluated at $t_{0.4}$

Pr Prandtl number, $\frac{c_p \mu g}{k}$

Re_b Reynolds number with density and viscosity evaluated at t_b, $\frac{\rho_b u_b D}{\mu_b}$

Re_0 Reynolds number with density and viscosity evaluated at t_0

$Re_{0.4}$ Reynolds number with density and viscosity evaluated at $t_{0.4}$

r_0^+ tube-radius parameter, $\frac{\sqrt{\tau_0/\rho_0}}{\mu_0/\rho_0} r_0$

t^+ static-temperature parameter, $\frac{(t_0 - t)c_p g \tau_0}{q_0\sqrt{\tau_0/\rho_0}} = \frac{1 - t/t_0}{\beta}$

t_b^+ bulk static-temperature parameter, $\frac{1}{\beta}\left(1 - \frac{t_b}{t_0}\right)$

t_1^+ value of t^+ at y_1^+

u^+ velocity parameter, $\frac{u}{\sqrt{\tau_0/\rho_0}}$

u_b^+ bulk velocity parameter, $\frac{u_b}{\sqrt{\tau_0/\rho_0}}$

u_1^+ value of u^+ at y_1^+

v $\frac{du^+}{dy^+}$

y^+ wall-distance parameter, $\frac{\sqrt{\tau_0/\rho_0}}{\mu_0/\rho_0} y$

y_1^+ value of y^+ at intersection of curves for flow close to wall and at a distance from wall

APPENDIX B

ANALYSIS INCLUDING EFFECT OF VARIATION OF SHEAR STRESS AND HEAT TRANSFER ACROSS TUBE (PRANDTL NUMBER = 1)

The following analysis was made to determine the effect of variation of shear stress and heat transfer across the tube on the velocity and temperature distributions with variable fluid properties. The variations of shear stress and heat transfer in the region close to the wall are negligible so that only the region at a distance from the wall is considered.

The relation for the variation of shear stress with radius for fully developed flow is obtained by equating the shear forces to the pressure forces acting on a cylinder of fluid of arbitrary radius and differential length. This relation gives

$$\tau = \tau_0 \left(1 - \frac{y}{r_0}\right) \tag{1B}$$

The heat transfer per unit area varies in approximately the same way as the shear stress, although the variation is not linear. For the purpose of determining the general effect of the variation of heat transfer, the following relation is assumed:

$$q = q_0 \left(1 - \frac{y}{r_0}\right) \tag{2B}$$

Substituting equations (1B) and (2B) into equations (1) and (2), dividing equation (2) by equation (1), and integrating the result between the wall and a point in the fluid give, for a Prandtl number of 1,

$$\frac{q_0 u}{c_p g \tau_0} = t_0 - t \tag{3B}$$

or

$$\frac{t}{t_0} = 1 - \beta u^+ \tag{4B}$$

With substitution of equations (4), (1B), and (4B), equation (1) can be written in dimensionless form with the molecular shear stress neglected as

$$\left(1 - \frac{y^+}{r_0^+}\right) = \frac{\varkappa}{1-\beta u^+} \frac{(du^+/dy^+)^4}{(d^2u^+/dy^{+2})^2}$$

or

$$\frac{d^2u^+}{dy^{+2}} = - \varkappa \frac{1}{\sqrt{(1 - \beta u^+)\left(1 - \frac{y^+}{r_0^+}\right)}} \left(\frac{du^+}{dy^+}\right)^2 \tag{5B}$$

where the negative sign was selected in taking the square root in order to make $\varkappa$ positive.

In order to solve equation (5B) let

$$\frac{du^+}{dy^+} = v \tag{6B}$$

Integration of equation (6B) gives

$$y^+ = y_1^+ + \int_{u_1^+}^{u^+} \frac{du^+}{v} \tag{7B}$$

With substitution of equations (6B) and (7B), equation (5B) becomes

$$\frac{dv}{v} = - \varkappa \frac{du^+}{\sqrt{(1 - \beta u^+)\left(1 - \frac{y_1^+}{r_0^+} - \frac{1}{r_0^+}\int_{u_1^+}^{u^+} \frac{du^+}{v}\right)}}$$

or

$$v = v_1 e^{-\varkappa \int_{u_1^+}^{u^+} \frac{du^+}{\sqrt{(1 - \beta^+)\left(1 - \frac{y_1^+}{r_0^+} - \frac{1}{r_0^+}\int_{u_1^+}^{u^+} \frac{du^+}{v}\right)}}} \tag{8B}$$

Equation (8B) can be solved by iteration by substituting assumed values for u^+ and v into the right side of the equation and calculating new values of v. After the relation between u^+ and v has been obtained for various values of β' and r_0^+, y^+ can be calculated from equation (7B).

APPENDIX C

ANALYSIS INCLUDING EFFECT OF MOLECULAR SHEAR STRESS AND HEAT TRANSFER IN REGION AT A DISTANCE FROM WALL (PRANDTL NUMBER = 1)

The effect of the molecular shear stress and heat-transfer terms in equations (1) and (2) on the velocity and temperature distributions is investigated in this section. When these terms are retained, the relation between temperature and velocity is given by equation (4B) as before. Equation (1) becomes, when written in dimensionless form for flow at a distance from the wall (Pr = 1),

$$1 = (1 - \beta u^+)^d \frac{du^+}{dy^+} + \frac{\varkappa^2 (du^+/dy^+)^4}{(1 - \beta u^+)(d^2u^+/dy^{+2})^2} \tag{1C}$$

For solving this equation let

$$\frac{du^+}{dy^+} = v \tag{2C}$$

Then

$$\frac{d^2u^+}{dy^{+2}} = \frac{dv}{dy^+} = v \frac{dv}{du^+}$$

As a result of substitution of these quantities in equation (1C)

$$\frac{dv}{v} = - \frac{\varkappa}{\sqrt{\left[1 - (1 - \beta u^+)^d v\right](1 - \beta u^+)}} du^+$$

As in equation (18) the negative sign was selected in taking the square root. Integration yields

$$v = v_1 e^{-\varkappa \int_{u_1^+}^{u^+} \frac{du^+}{\sqrt{\left[1 - (1 - \beta u^+)^d v\right](1 - \beta u^+)}}} \tag{3C}$$

where the subscript 1 indicates that the values of u^+ and v are at the lowest value of y^+ for which the equation applies. By assuming values of v corresponding to values of u^+ and then calculating new values of v by numerically integrating the right side of the equation, equation (3C) can be solved by iteration. After the relation between u^+ and v has been obtained from equation (3C), the relation between u^+ and y^+ can be obtained by integrating equation (2C) as follows:

$$y^+ = y_1^+ + \int_{u_1^+}^{u^+} \frac{du^+}{v} \qquad (4C)$$

where y_1^+ is the lowest value of y^+ for which equation (1C) applies.

REFERENCES

1. Humble, Leroy V., Lowdermilk, Warren H., and Desmon, Leland G.: Measurements of Average Heat Transfer and Friction Coefficients for Subsonic Flow of Air in Smooth Tubes at High Surface and Fluid Temperatures. NACA Rep. 1020, 1951. (Formerly RM's E7L31, E8L03, E50E23, and E50H23.)

2. Deissler, Robert G.: Analytical Investigation of Turbulent Flow in Smooth Tubes with Heat Transfer with Variable Fluid Properties for Prandtl Number of 1. NACA TN 2242, 1950.

3. Deissler, Robert G.: Analytical and Experimental Investigation of Adiabatic Turbulent Flow in Smooth Tubes. NACA TN 2138, 1950.

4. Bernardo, Everett, and Eian, Carroll S.: Heat-Transfer Tests of Aqueous Ethylene Glycol Solutions in an Electrically Heated Tube. NACA ARR E5F07, 1945.

5. Deissler, Robert G.: Analytical Investigation of Fully Developed Laminar Flow in Tubes with Heat Transfer with Fluid Properties Variable Along the Radius. NACA TN 2410, 1951.

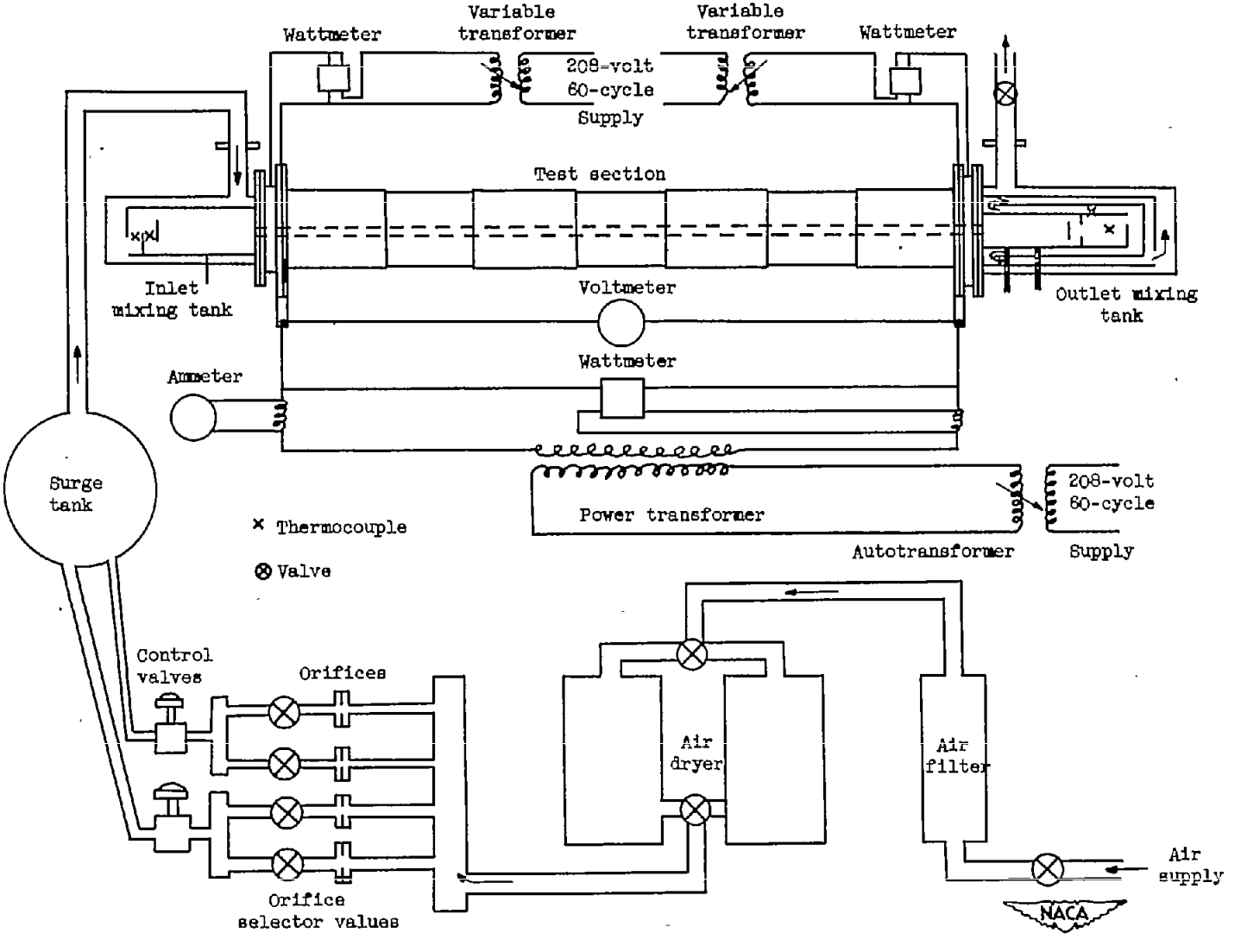

Figure 1. - Schematic diagram showing arrangement of apparatus.

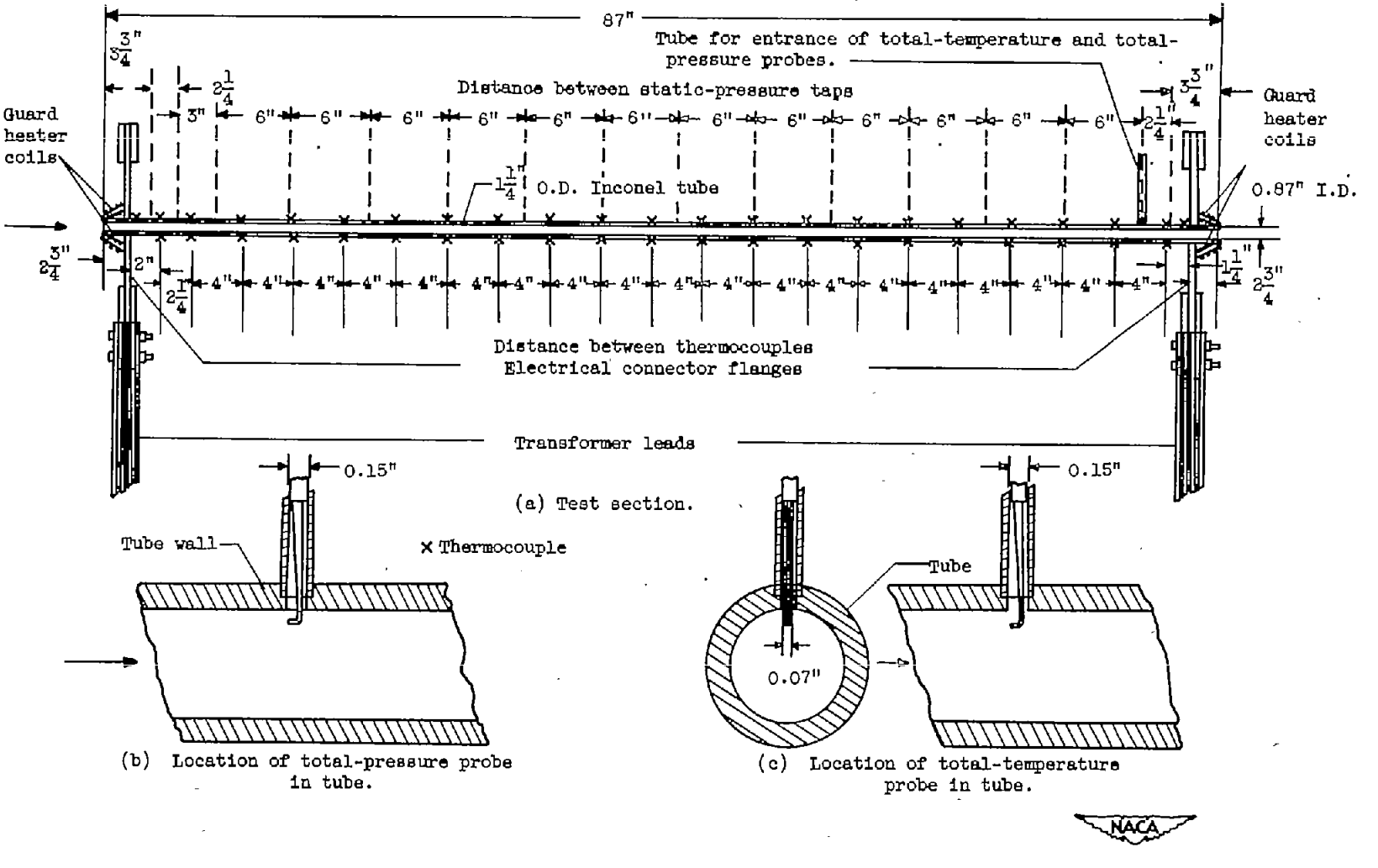

Figure 2. - Test section and probes.

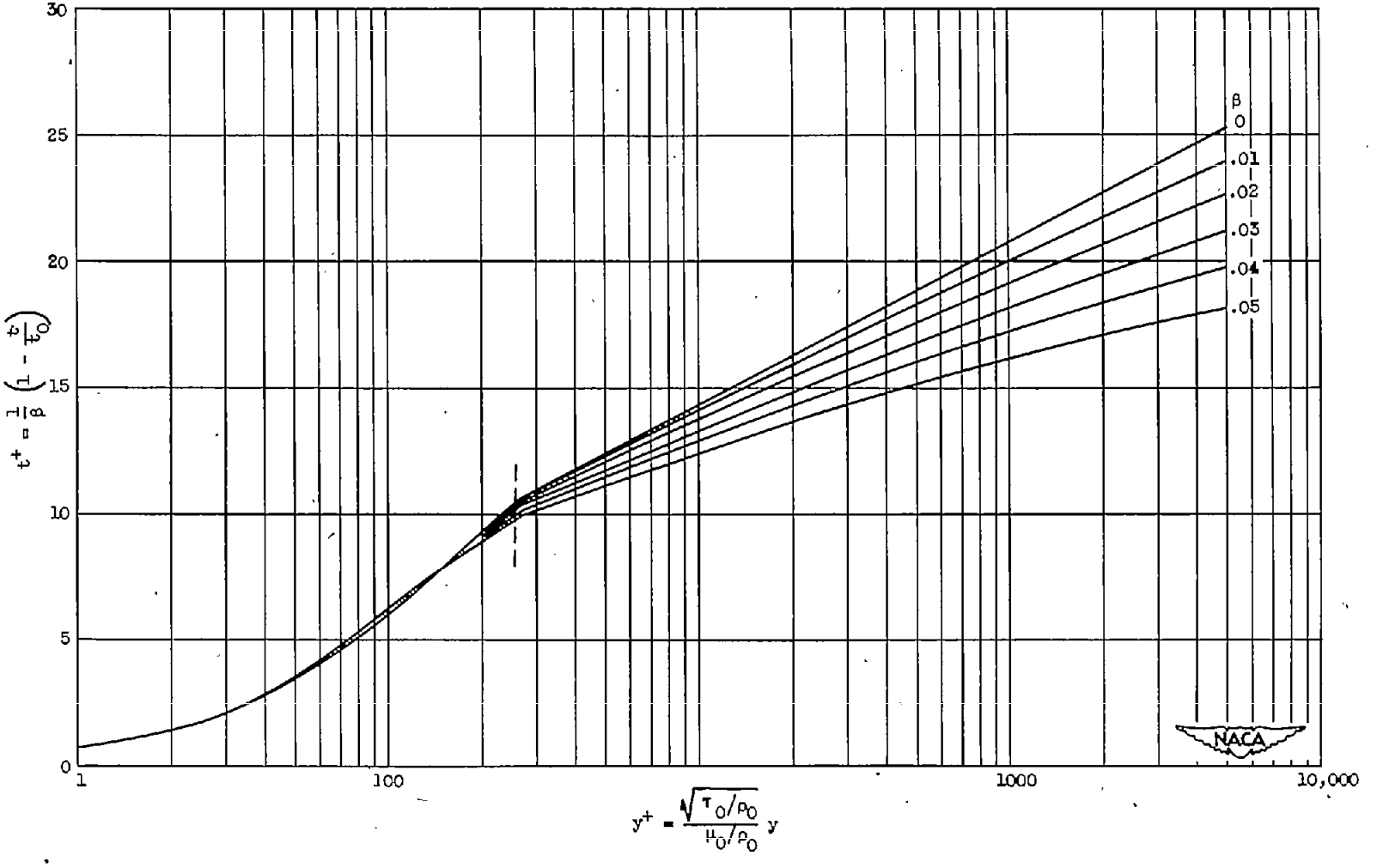

Figure 3. - Predicted generalized temperature distribution for flow of gases with heat addition at Prandtl number 0.73.

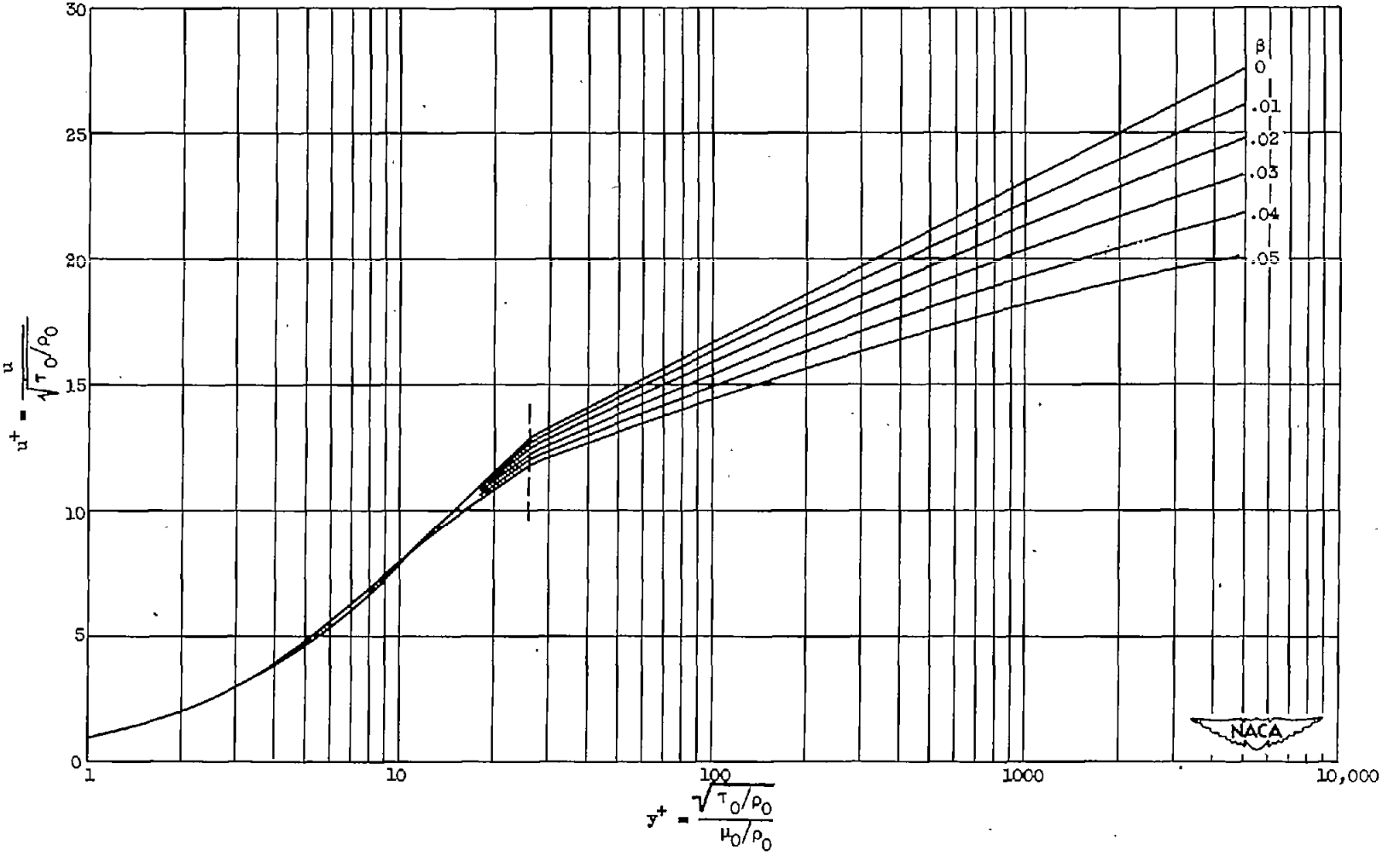

Figure 4. - Predicted generalized velocity distribution for flow of gases with heat addition at Prandtl number 0.73.

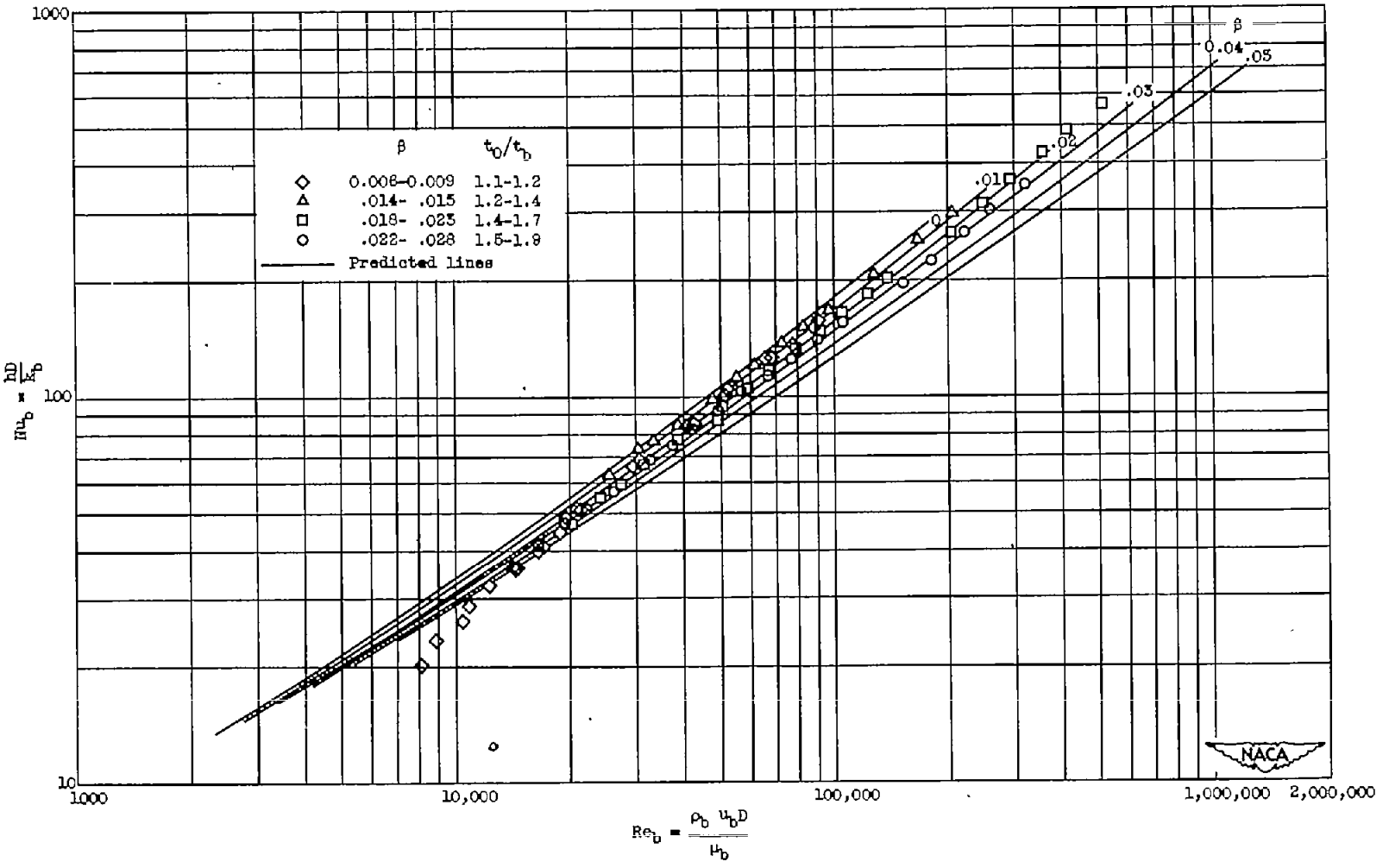

Figure 5. - Variation of Nusselt number with Reynolds number for flow of air with heat addition and properties evaluated at static bulk temperature. Prandtl number, 0.73.

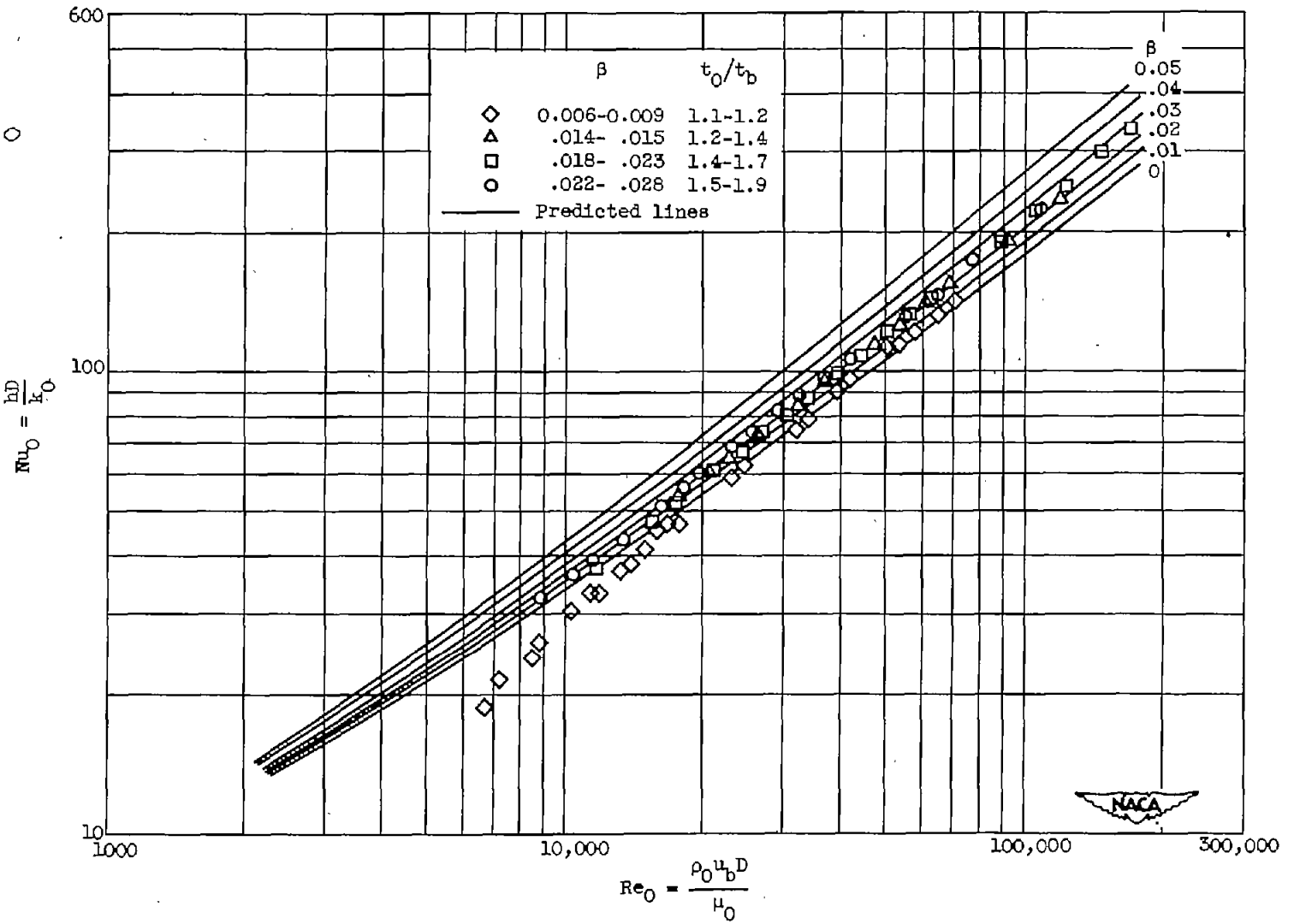

Figure 6. - Variation of Nusselt number with Reynolds number for flow of air with heat addition and properties evaluated at tube-wall temperature. Prandtl number, 0.73.

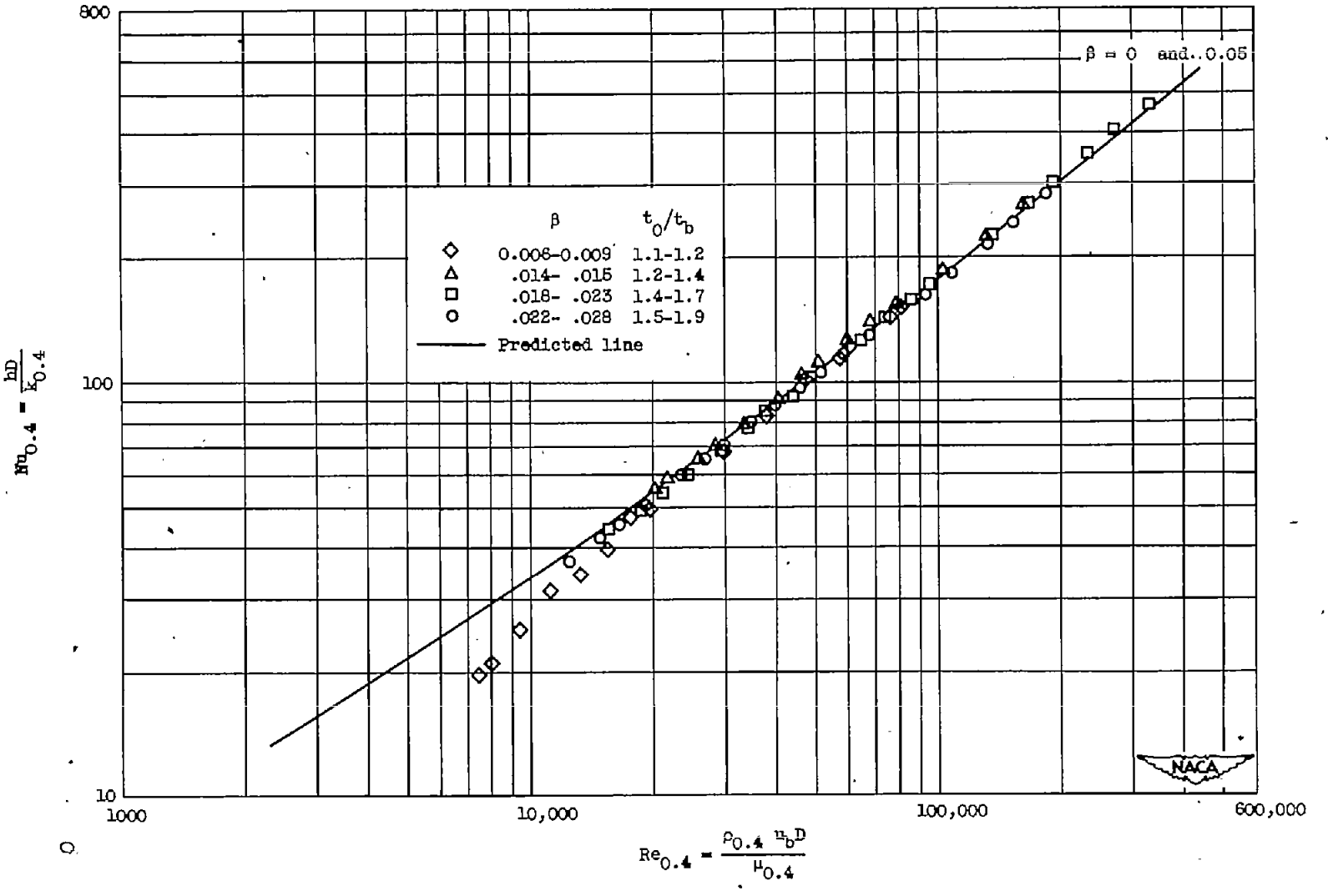

Figure 7. - Variation of Nusselt number with Reynolds number for flow of air with heat addition and properties evaluated at $t_{0.4} = 0.4 (t_0 - t_b) + t_b$. Prandtl number, 0.73.

Figure 8. - Variation of friction factor with Reynolds number for flow of air with heat addition and properties evaluated at $t_{0.4} = (t_0 - t_b) + t_b$. Prandtl number, 0.73.

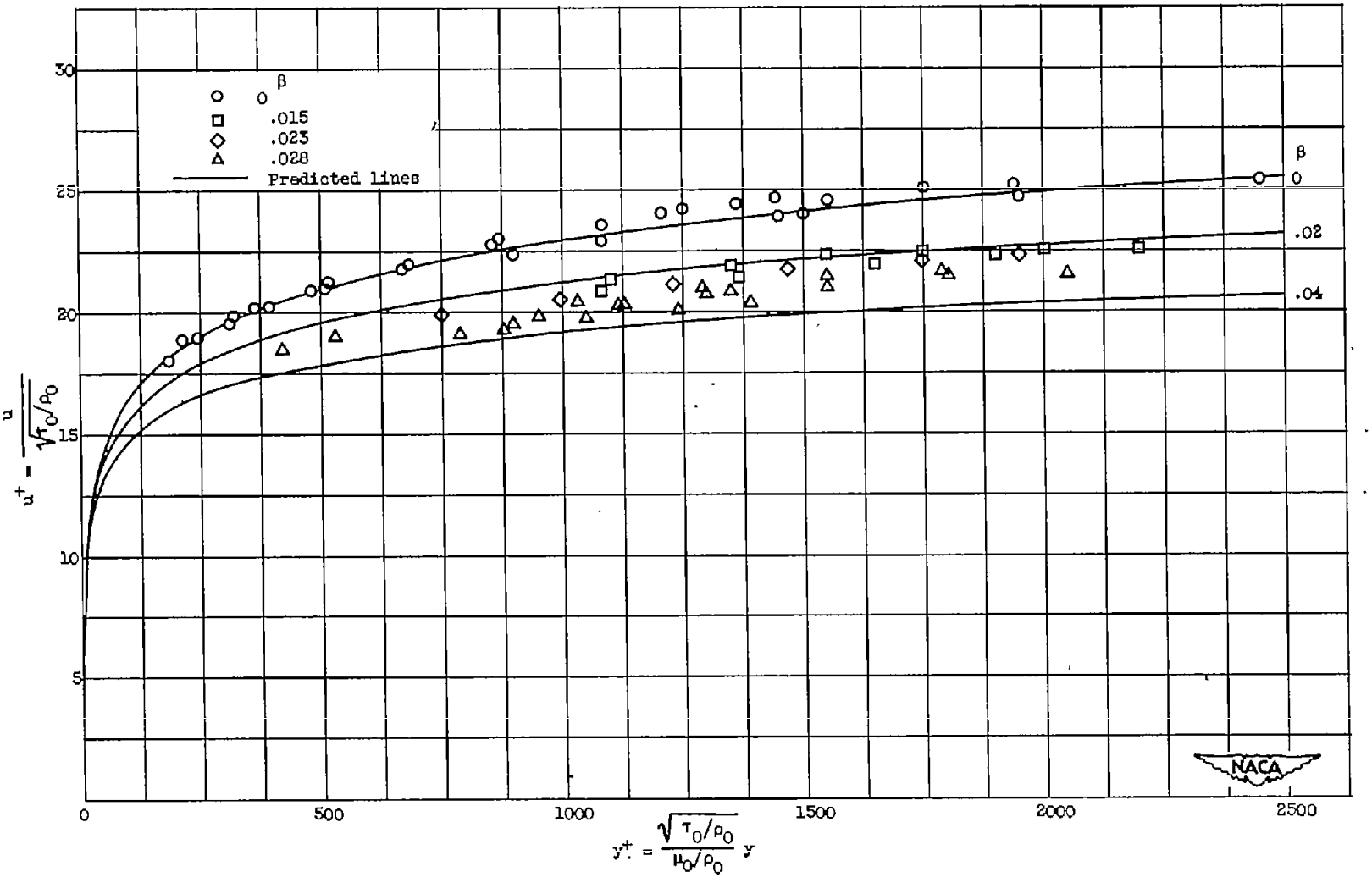

Figure 9. - Generalized velocity distribution for flow of air with heat addition. Prandtl number, 0.73; Reynolds numbers for data, 100,000-250,000.

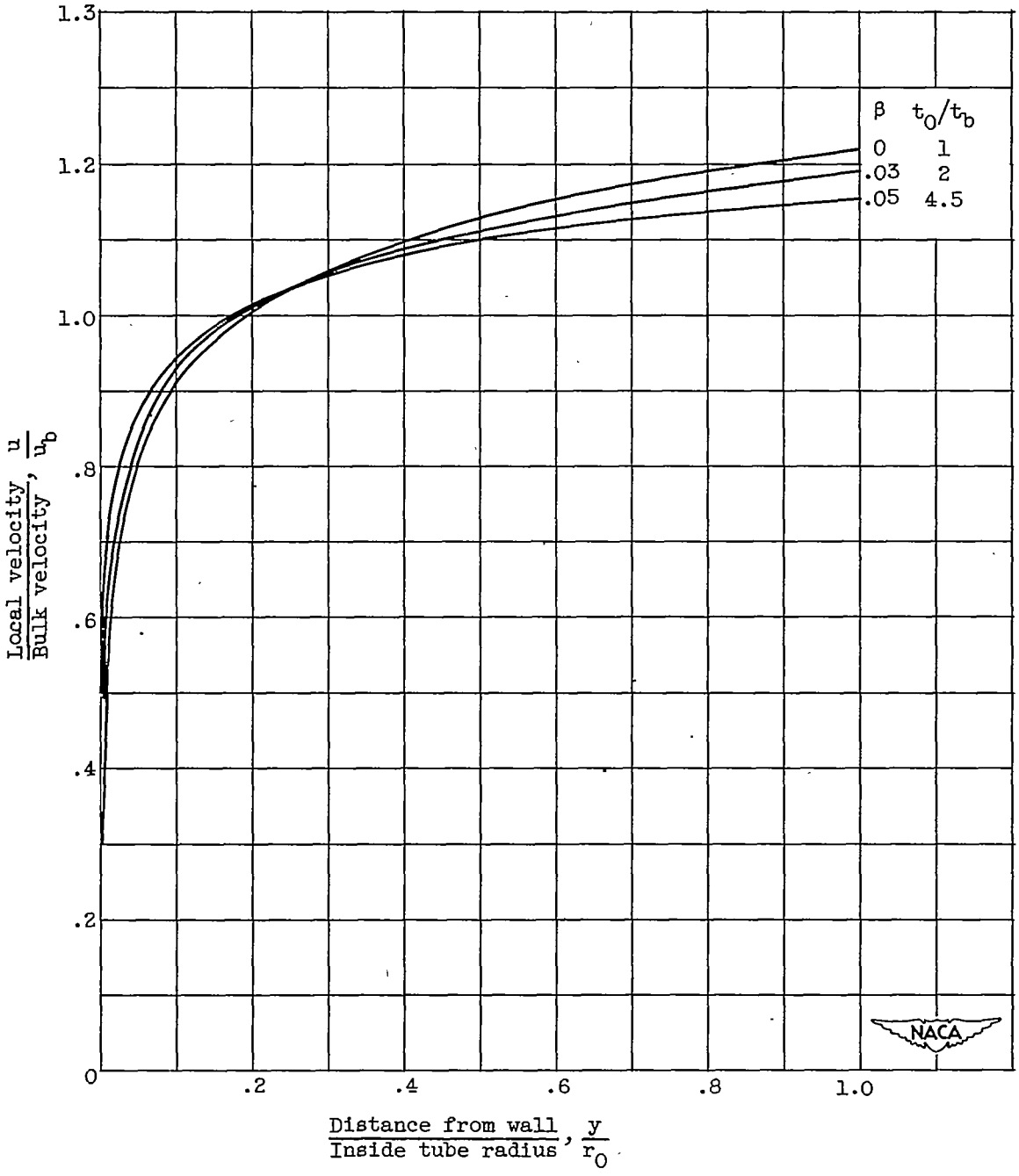

Figure 10. - Predicted effect of heat transfer on shape of velocity profile. Tube-radius parameter r_0^+, 2000; Prandtl number, 0.73.

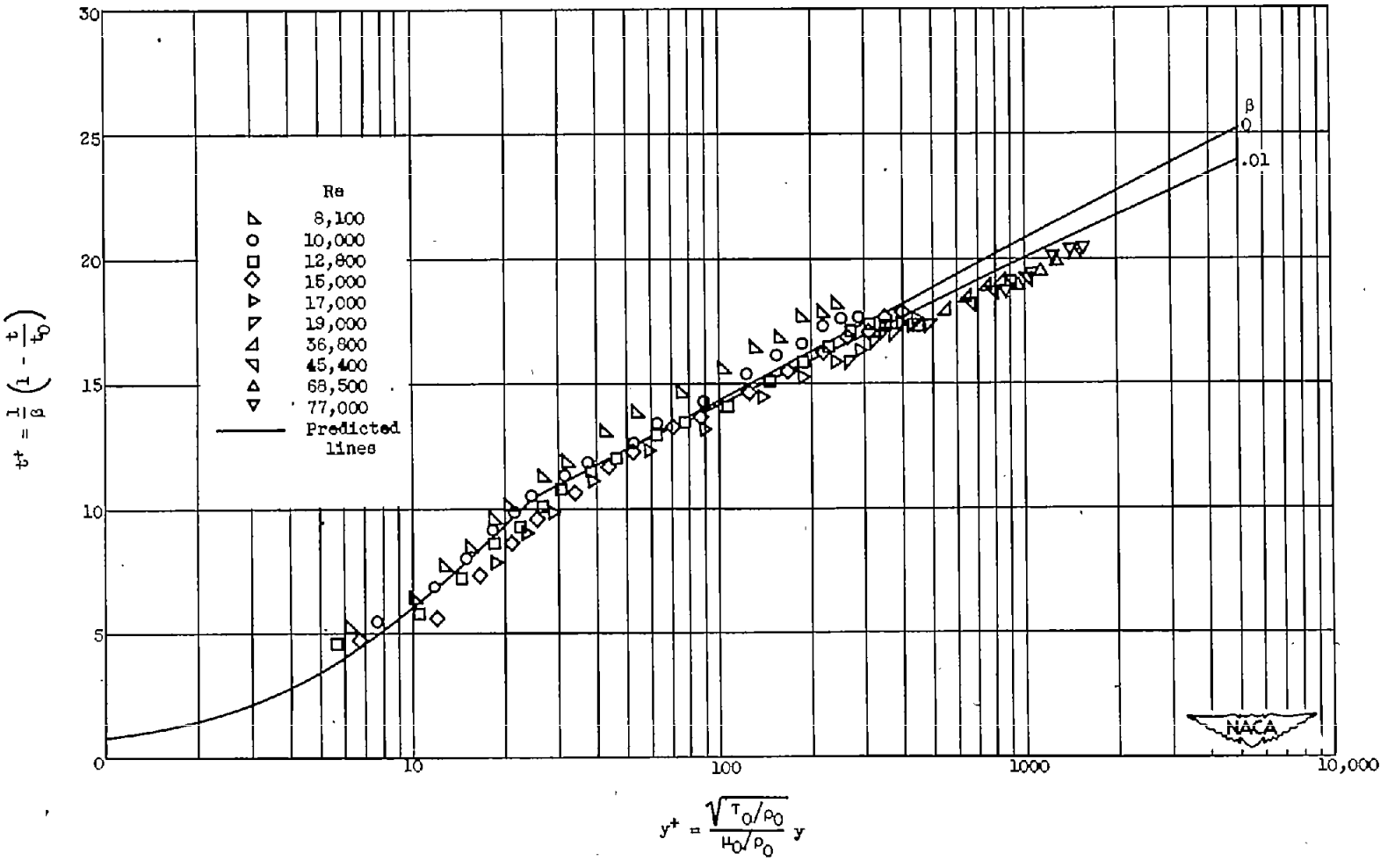

Figure 11. - Generalized temperature distribution for flow of air with low rates of heat addition. Prandtl number, 0.75; β for data, 0.0075-0.0093; t_0/t_b for data, 1.1-12.

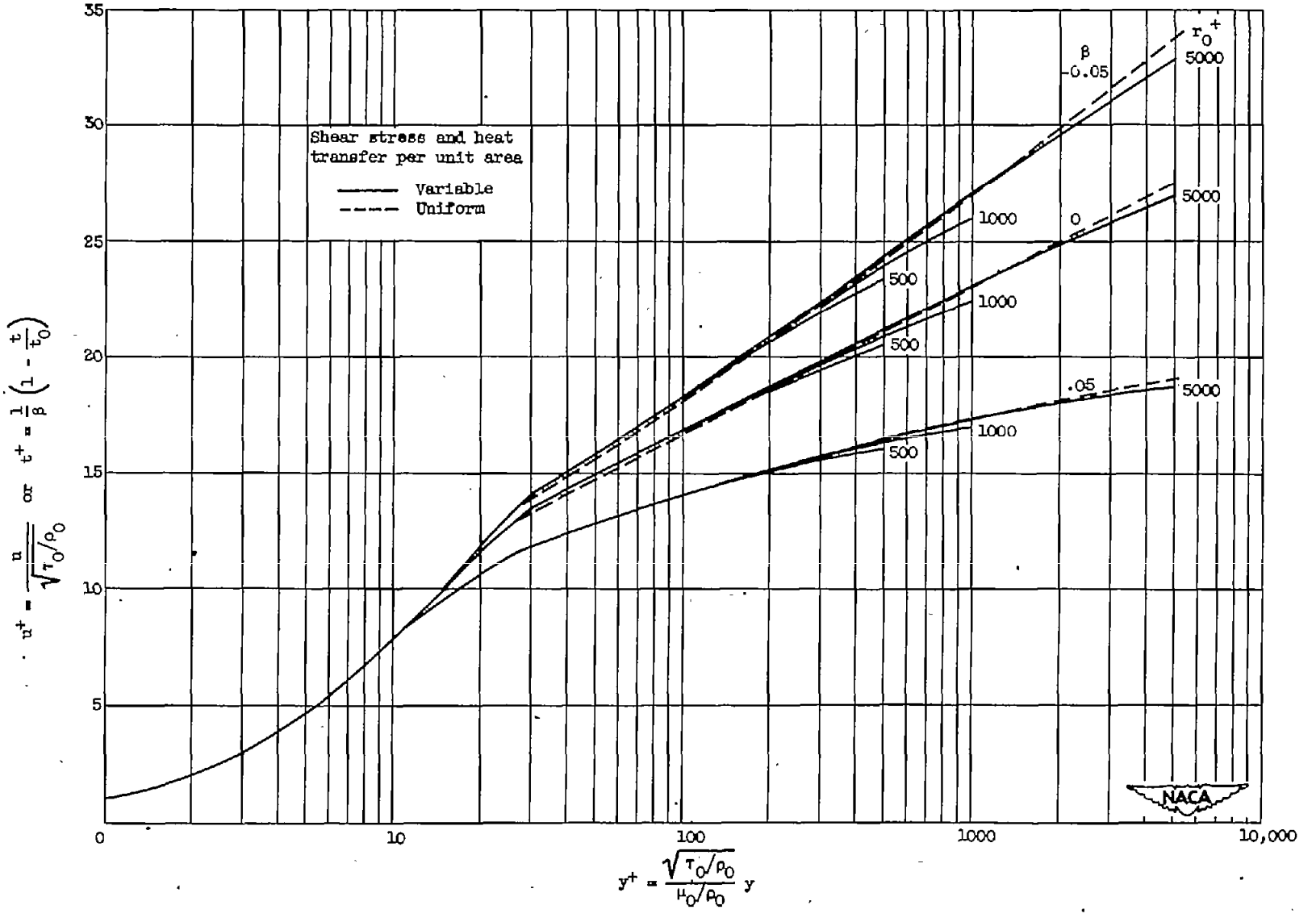

Figure 12. - Curves showing predicted effect of variation of shear stress and heat transfer across tube on velocity and temperature distributions of gases. Prandtl number, 1.

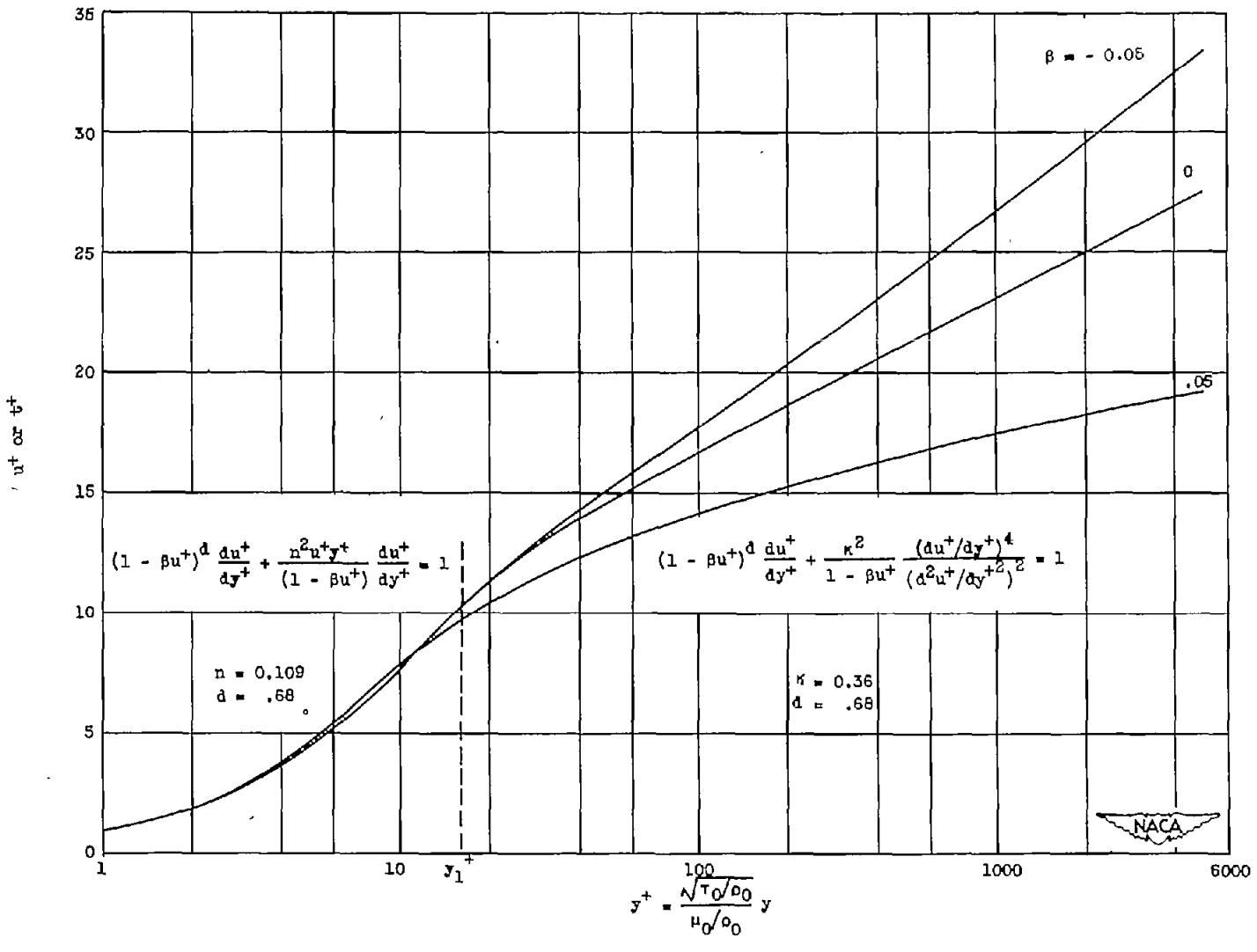

Figure 13. - Generalized velocity or temperature distribution for turbulent flow of gases with heat transfer, variable fluid properties, and molecular shear stress and heat transfer considered in region at distance from wall. Prandtl number, 1.

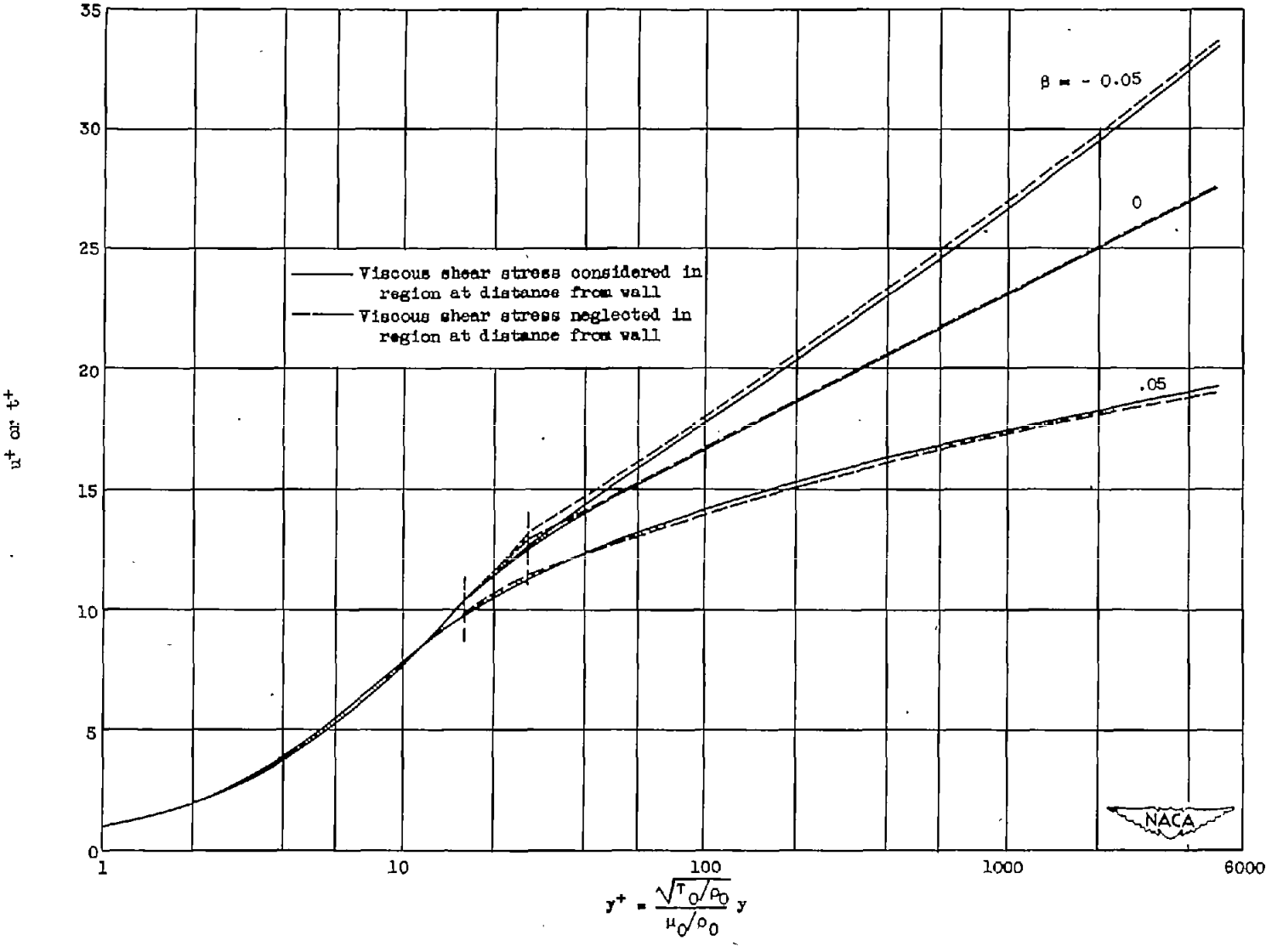

Figure 14. - Curves showing effect of neglecting molecular shear stress and heat transfer in region at distance from wall.